ACS APPLIED MATERIALS & INTERFACES

Research Article

www.acsami.org

Redox-Switchable Copper(I) Metallogel: A Metal–Organic Material for Selective and Naked-Eye Sensing of Picric Acid

Sougata Sarkar,[†] Soumen Dutta,[†] Susmita Chakrabarti,[‡] Partha Bairi,[§] and Tarasankar Pal*[,†]

[†]Department of Chemistry, Indian Institute of Technology, Kharagpur 721302, India

[‡]Department of Chemistry, Jadavpur University, Kolkata 700032, India

[§]Polymer Science Unit, Indian Association for the Cultivation of Science, Kolkata 700032, India

Supporting Information

ABSTRACT: Thiourea (TU), a commercially available laboratory chemical, has been discovered to introduce metallogelation when reacted with copper(II) chloride in aqueous medium. The chemistry involves the reduction of Cu(II) to Cu(I) with concomitant oxidation of thiourea to dithiobisformamidinium dichloride. The gel formation is triggered through metal–ligand complexation, i.e., Cu(I)-TU coordination and extensive hydrogen bonding interactions involving thiourea, the disulfide product, water, and chloride ions. Entangled network morphology of the gel selectively develops in water, maybe for its superior hydrogen-bonding ability, as accounted from Kamlet–Taft solvent parameters. Complete and systematic chemical analyses demonstrate the importance of both Cu(I) and chloride ions as the key ingredients in the metal–organic coordination gel framework. The gel is highly fluorescent. Again, exclusive presence of Cu(I) metal centers in the gel structure makes the gel redox-responsive and therefore it shows reversible gel–sol phase transition. However, the reversibility does not cause any morphological change in the gel phase. The gel practically exhibits its multiresponsive nature and therefore the influences of different probable interfering parameters (pH, selective metal ions and anions, selective complexing agents, etc.) have been studied mechanistically and the results might be promising for different applications. Finally, the gel material shows a highly selective visual response to a commonly used nitroexplosive, picric acid among a set of 19 congeners and the preferred selectivity has been mechanistically interpreted with density functional theory-based calculations.

KEYWORDS: *thiourea, metal–organic gel, copper(I), redox-switchability, picric acid sensing*

INTRODUCTION

Selective detection of commercial nitroexplosives is a major security concern in defense sectors and also an environmental issue.[1] Different research groups are actively engaged in their detection through the implementation of a variety of strategies which are good enough for trace level detection of the targeted explosives but in all cases they are somehow dependent on analytical instrumentations. Hence there is still challenge in low-cost fabrication of a material for naked eye detection of the nitroexplosive leaving aside the instrumental analysis for immediate response. Also, different substrates ranging from nanomaterials to supramolecular polymers have been investigated in this perspective,[1−15] though the use of gel and metal–organic framework-based materials[16−26] is still very limited. These gels, a kind of the soft functional materials having nanoscale morphologies, are continuously gaining increasing attention because of their promising applications in different branches of science and technology including catalysis, sensing, selective separation, sorption, optoelectronics, magnetism, drug delivery, environmental pollution abatement, and so on.[27−36] The past decade has seen the making of successful attempts in the designed fabrication of these supramolecular gels having intriguing properties.[37,38] Again, there are also reports on metal nanoparticle-embedded gels where the pristine soft materials serve as a suitable matrix for synthesis, encapsulation, and stabilization of the nanoparticles.[39−42] These nanoparticle–gel assemblies show fascinating physicochemical behaviors and have been used for a wide variety of applications.[39−42]

It has been anticipated that the regularly observed three-dimensional entwined fibrillar networks of the gels are originating from spontaneous participation of different coordinative and supramolecular interactions among the gelators through entrapment of large volume of solvent molecules. Clever monitoring of these couple of interactions has been successfully achieved through engineered design of

Received: November 6, 2013
Accepted: April 21, 2014
Published: April 21, 2014

   dx.doi.org/10.1021/am501491u | ACS Appl. Mater. Interfaces 2014, 6, 6308–6316

suitable organic molecules and in this context the so-called low-molecular-weight-gelators (LMWGs) are the most promising candidates.[43,44] Metallogels, are usually made up with metal ions and suitably designed organic ligands. The metal ions assisted gelation in-turn promotes the integration of physicochemical behaviors of the ions in the gel matrix.[45] And the ligands having a definite structural backbone formulate suitable synthons for the rational design of metal−ligand coordination building units and therefore stimulate the self-assembly in a convenient manner. Though there are several reports on the design and synthesis of new and interesting ligand systems to commence the metallogelation in suitable solvents, comparatively little efforts have been made with the implementation of commercially available organic molecules in making such a metallogel assembly.[46−52]

These metal−ligand coordination complexes are grown-up and stabilized with an assortment of several essential regulating parameters for example hydrogen bonding, metal−ligand coordination, ions, pH, solvent composition, temperature etc. and therefore the organized assembly is frequently perturbed when making a change in either of one or more of these variables by any means. This perturbation causes physical or chemical alterations of the framework and a set of specific stimuli that are shown to be responsible to make the gel stimuli responsive in nature.[53,54] This study is receiving tremendous attention these days in research with the soft materials because of the intriguing information associated with the behavior of the gels in a definite chemical environment. For example, the presence of redox-active metal centers has introduced a newer dimension and was first reported by Shinkai et al.[55] in a Cu(I) containing gel of 2,2′-bipyridine derived ligand. Another report on a cholesterol-appended ferrocenyl metallogel was observed to show similar reversible redox-responsive performances. There are other very few reports on such fascinating metallogel.[56−58] This leaves a scope to explore the redox-switchable behavior in the case of a suitably designed metallogel.

The current study represents the formation of a metallogel when thiourea reacts with copper(II) chloride in aqueous solution in a definite molar equivalent ratio. The reaction is driven by spontaneous reduction of Cu(II) to Cu(I) and subsequent oxidation of thiourea to a disulfide product. The thiourea−Cu(II) solution chemistry is age-old[59] but the formation of a metallogel has never been looked into from this duo. The observed formation of the entangled networks is principally driven by metal−ligand coordination and hydrogen bonding interactions. The gel formation is highly selective toward Cu(II) and chloride ions. Cu(II) salts with other counteranions (except bromide as $CuBr_2$ could also results gelation) and no other metal chloride salts could bring this gelation. Solvent effect study suggests the superiority of water as the most desired solvent system to favor the gelation process. The synthesized material was fluorescent in nature,[60] and it shows multiresponsive behavior to different stimuli. Finally, the presence of Cu(I) centers within the gel frameworks has turned the gel redox-responsive and hence, we could easily achieve gel−sol reversible phase transition repetitively with the exploitation of classical redox chemistry.

The most striking feature of the gel was noticed when it showed visual response selectively toward picric acid among other 18 electron deficient congeners. Picric acid, when introduced into the gel matrix, produces an orange-red precipitate even in its low concentration. Therefore, with thiourea and $CuCl_2$, we have synthesized a redox-switchable Cu(I) gel material in aqueous solution, which selectively responds to picric acid and thus provides a scope for naked-eye sensing of the commercial nitroexplosive, picric acid.

RESULTS AND DISCUSSION

Among the class of responsible ligands allowing metallogelation, urea-based gelators have been playing a major role and has been well-documented by Steed et al. and also by other research groups.[61−63] In comparison, the chemistry of thiourea derived ligands has been explored a little[64] and thus provides a wide scope in the development of new metallogelators. In our recent study with 2-mercaptobenzimidazole (2-MBIm)[52] we observed an instantaneous gelation of the ligand with copper(II) chloride in methanolic solution. After careful insight into the molecular structure of 2-MBIm, we revealed the presence of a thiourea-like binding site in its structural backbone (as indicated by red color in the thione tautomeric form of 2-MBIm in Figure 1). As the molecule also

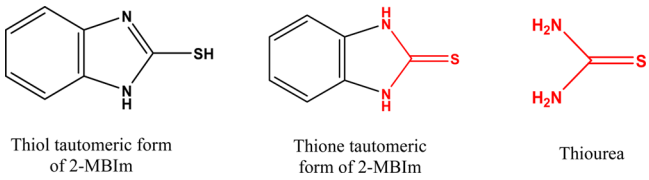

Figure 1. Thiol and thione tautomeric forms of 2-mercaptobenzimidazole showing the presence of "thiourea-like" binding site in the molecular structure.

instantaneously forms a metallogel with $CuCl_2$ (as observed in our previous MS), the simple thiourea molecule might also trigger gel formation with $CuCl_2$. Hence the above concept of introducing only thiourea molecule in the gel formation reaction with $CuCl_2$ is from our previous report,[52] and then we have deliberately examined the above idea and we succeeded to obtain a gel through reaction of thiourea and $CuCl_2$ in water. We observed that when an aqueous solution of thiourea (1 mL; 0.04 mmol) was reacted with an aqueous solution of copper(II) chloride (1 mL; 0.04 mmol) there was an immediate formation of a yellowish-green color solution that spontaneously turned into a white color opaque solution and ultimately resulted in a white colored gel upon standing for 1−2 h.

Figure 2 presents the feedback of the above reaction when we have made a variation in the concentration (equivalent) of added $CuCl_2$. We noticed that every added equivalent of $CuCl_2$ was not equally capable to introduce metallogelation. Stable gel formation was observed up to 0.5 mol equiv. of $CuCl_2$ (i.e., up

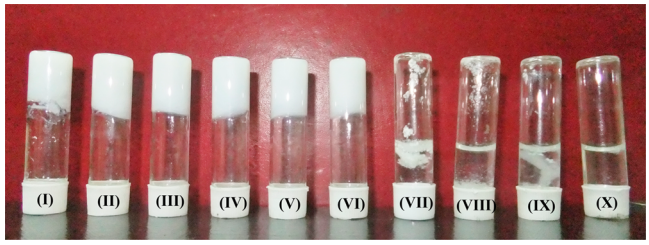

Figure 2. $CuCl_2$−thiourea complex as metallogel with variation in $CuCl_2$ molar equivalent from 1.0−0.1 w.r.t. molar equivalent of thiourea (From set I to set X).

dx.doi.org/10.1021/am501491u | ACS Appl. Mater. Interfaces 2014, 6, 6308−6316

to set VI) as indicated by "inversion of the glass vial" method. In contrast, the gels or rather the viscous materials for sets VII–VIII (i.e., up to 0.3 mol equiv) flow freely. This feature indicates the partial/weak gelation resulting from the less population of the formed gel fibers in the reaction medium. And finally no such gel formation was observed when 0.2 and 0.1 mol. equiv. of $CuCl_2$ were introduced (i.e., for set IX and X). Rather a little white precipitate was slowly formed for these sets. Hence the minimum total weight percentage of $CuCl_2$ and thiourea required to form the gel is 0.245*g*/100 mL. Therefore, the "Cu(II)/thiourea" ("Cu/TU" hereafter) stoichiometry has a critical influence on the states of the metallogelation. The key role of metal ion/ligand ratio in the process of gelation has been described also by other research groups[50] The as-prepared gel was stable and shows no marked visible change for couple of months. The gel obtained from set I "Cu/TU" molar ratio was selected for further studies. Here it is worth mentioning that similar gelation could be achieved with $CuBr_2$ in lieu of $CuCl_2$.

Figure 3 represents the typical FESEM images of the as-synthesized metallogel of set I (Cu/TU molar ratio 1). The

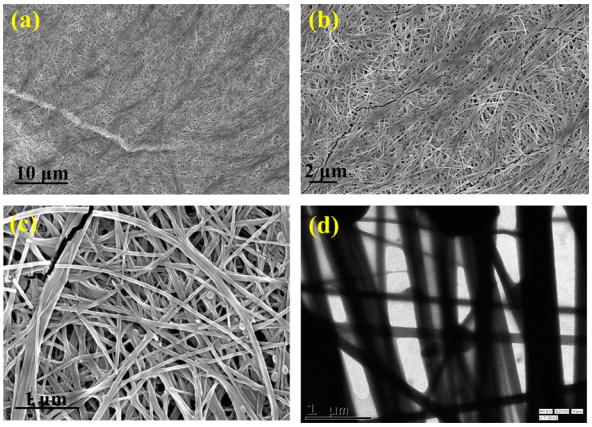

Figure 3. FESEM images of the metallogel (set I) at (a) low, (b) medium, and (c) higher magnifications; (d) TEM image of the metallogel (set I).

panoramic image in Figure 3a is an overview of the dense fibrillar network. The high-yield grown morphology is favorably composed of intertwined nanofibers that spontaneously self-assemble to form the three-dimensional (3D) architectures. The fibers are several micrometers long and have an approximate width of ∼100 nm. Somewhere the individual fibers are observed to assemble concurrently to result in bundled aggregates (Figure 3b). Again, the simultaneously occurring straight and bending morphology of the nanowires indicate their structural flexibility (Figure 3c). The cross-linked network structure is also evident from the TEM image of the material (Figure 3d). The fibers are of higher aspect ratio and form the 3D network. Successive FESEM images of the materials for other sets with varied Cu/TU equivalent ratio are presented in Figure S2 in the Supporting Information. Surprisingly, no major morphological alterations were noticed among the images. Fibrous aggregates were commonly observed to occur in every cases. The EDAX pattern and mapping of the metallogel confirm the presence of Cu, Cl, S, and N as the key compositional elements of the hybrid material (see Figure S3 in the Supporting Information). Again the similar entangled feature is also obvious from the FESEM image of the xerogel (see Figure S4 in the Supporting Information). The birefringent nature of the gel fibers is clear from the polarized optical microscopic image (see Figure S5a in the Supporting Information) and results from their highly anisotropic structural characteristics. Similar microscopic features are again observed but for the bromide analogue (see Figure S5b–e in the Supporting Information).

In a similar reaction environment, no such gelation was observed with other Cu(II) salts like perchlorate, nitrate, sulfate, and acetate. Here, they form a clear solution or quickly results some insoluble species (for acetate only). These observations thus concluded the necessity of $CuCl_2/CuBr_2$ in the gelation process.

The above study thus substantiated the essential requirement of chloride/bromide ion in association with Cu^{2+} in the event of gelation. This proposition was absolutely supported with the evidence that external addition of any ionizable chloride/bromide salt or even HCl/HBr (of definite equivalent concentration) to a clear solution mixture of $Cu(ClO_4)_2$ and thiourea could also make the metallogel. But fluoride ion could not bring any chemical and physical change in the material and practically remains inert in this case. The results thus authenticate the crucial participation of chloride/bromide ion in the gel-making recipe. A recent observation by Džolić et al. has reported the favorable formation of metallogel by a pyridyloxalamide based gelator only with $CuCl_2$. No other Cu(II) salts were able to make the gel.[65] Similarly Lee et al. has presented the successful formation of Ag(I) metallogel of a tetrazole appended gelator only for ClO_4^- and NO_3^- counterions, whereas CH_3COO^- and SO_4^{2-} analogues failed to do so.[66]

In a true sense, the solution chemistry of the duo (thiourea and Cu^{2+} salt) always leads to a spontaneous one-electron reduction of the Cu(II) to Cu(I) with concomitant oxidation of thiourea to α,α'-dithiobisformidinium dichloride.[59] A series of mono/polynuclear structures have been reported in literature with diverse anions. Assessment of the related crystal structures reveals a tetrahedral geometry of the Cu(I) centers where thiourea molecule acts as the coordinating ligand through its sulfur atom.[59] This coordination may be terminal or bridging though the latter mode is preferably observed in our case. In such way the "CuS_4" motif forms dimeric/trimeric/oligomeric units. These units are held together with different types of hydrogen bondings where the N–H protons from the NH_2 functional (of coordinated thiourea and the oxidized dithio product) are the key ingredient to it. This offers the favorable creation of N–H···S and N–H···Cl hydrogen bonds throughout the entire structure. Again the solvent water molecules also participate in the weak-force interactions. These extensively extended hydrogen bonds thus ultimately make the supramolecular gel assembly. Now it is anticipated that this polymeric structure indeed offers a suitable compartment to gluing the Cl^- ions through hydrogen bonding. As illustrated by Bombicz et al.,[59] the Cl^- ions experience a hepta-coordination mode of hydrogen bonding in a related structure. This host–guest interaction is principally controlled by the size of the anion which can now explain the chloride ion selective gel formation. It is obvious that here other anions (ClO_4^-, SO_4^{2-}, NO_3^-, CH_3COO^-) are not encapsulated because of their size parameter. Such anion selectivity in the fabrication of supramolecular metallogel has been delicately presented for diverse urea functional gelators by Steed at al.[67] In contrast to the anion dependency, no other metal chloride/bromide salts were similarly able to make any gel under the same reaction

environment. Here it is worth noting that only Cu(I) could not form gel directly with thiourea. Therefore, simultaneous presence of both Cu(II) and Cl^-/Br^- ions were essential to achieve the metallogel formation.

The gelation was studied only in a couple of polar protic and aprotic solvents due to the insolubility of the gelators in other nonpolar solvent. As already observed, the gelation could be always achieved in H_2O. But for methanol, acetonitrile, butanol, octanol, pentanol, and dimethylformamide, formation of curdy precipitates or a clear solution was observed. It is recommended that large volumes of solvent water molecules are trapped in the interstitial sites of assembled nanofibers and directs the gel formation. The favor toward H_2O can be explained with Kamlet–Taft solvent parameters,[68] which describes the superior engagement of the water molecules in extensive formation of hydrogen bonding through its higher α (hydrogen bond donation ability) value (α = 1.17).

The gel shows thermo-irreversible behavior when heated and finally converted into a greenish-blacky substance. The thermogram is shown in Figure S11 in the Supporting Information.

The presence of Cu(I) centers made our as synthesized gel highly redox-responsive. Accordingly, the gel gets dissolved upon gradual addition of ferric chloride solution and results in a clear greenish-yellow solution. And surprisingly, slow addition of an equivalent molar quantity of ascorbic acid (AA) instantaneously initiates the reductive gel formation through continuous fading of the greenish coloration and finally the white gel completely reverts back. Figure 4 presents the

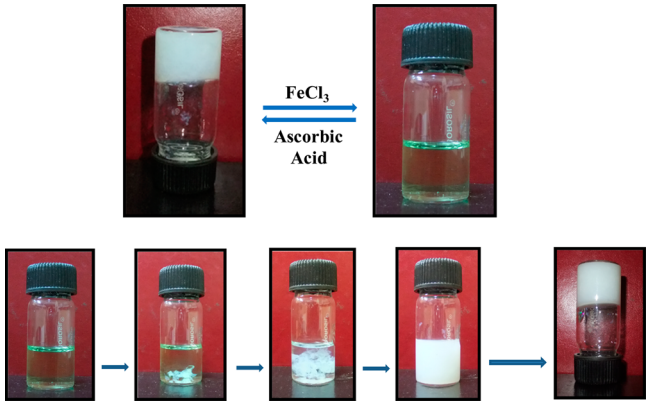

Figure 4. $FeCl_3$–ascorbic acid mediated redox-switchable gel–sol reversible phase transition of synthesized $CuCl_2$–thiourea metallogel system (upper panel) and gradual addition of ascorbic acid promotes regeneration of the gel material from the oxidized sol phase (lower panel).

oxidative dissolution and reductive regeneration of the gel matrix. Here it is worth mentioning that the redox-switchable gel–sol transition happens in room temperature and can be performed repeatedly. The respective FESEM images (Figure 5) clearly indicate that the network morphology absolutely dissolves out upon oxidation and again reappears upon reduction. This Fe(III) mediated Cu(I)/Cu(II) reversible redox chemistry could also be turned on with an aqueous acidic (HCl) solution of potassium dichromate in lieu of $FeCl_3$ where Cr(VI) is reduced to Cr(III) (see Figure S12 in the Supporting Information). Again, the morphology remains unaltered upon AA made regeneration of the gel. Here it is important to note that AA only acts as the reducing agent to

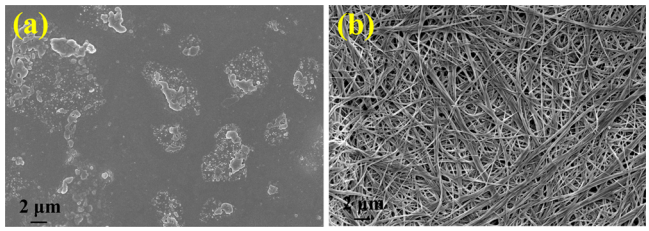

Figure 5. FESEM images of the (a) oxidized sol and (b) regenerated gel materials indicating the crucial role of Cu(I) ions in making the nanoscale gel framework.

revert backs the gel phase from the oxidized sol phase, i.e., AA helps only in reducing the Cu(II) ions (present in the oxidized sol phase) to the Cu(I) and it has no other function in the gel formation. We have also employed other oxidizing agents like $NOBF_4$ but this renders the oxidation of the sulfur containing ligand also along with the Cu(I) centers and thus the reversibility is lost. Thus, from the above intrinsic characteristics of the Cu(I) metallogel, it is readily understandable that the oxidation state of the metal centers have an essential role in controlling the stability of the metallogel.

At room temperature, facile electron transfer from the gel matrix to oxidizing agents specifies the material as an electron-rich platform and prompted us to examine the fate of electron deficient molecules when they are in association with this material. For this we have introduced 19 different compounds (nitro and others) individually. Figure 6 presents the pictorial representation of the as prepared gel material but in the presence of an ethanolic solution of the selected species (concentration = 0.01 M). Surprisingly enough, we noticed the formation of an orange-red precipitate only with picric acid. And no obvious change in the color of the metallogel was observed with the rest of the entries. Such exceedingly selective response of the gel system toward a commonly used explosive over a series of others then encouraged us to study the interactions of this trinitrophenol derivative with the Cu(I) containing gel material in detail.

Figure 7 presents the consequence of addition of varied concentration (50 mM to 50 μM) of picric acid solution in the gel matrix. As clearly observed, there was formation of the orange-red stuff even with 2.5 mM picric acid solution with subsequent breaking of the metallogel. The other diluted concentrations either initiate a yellow coloration or cannot bring any noticeable visible changes to the matrix.

This picric acid initiated disintegration also caused a complete morphological change of the robust fibrillar architectures as indicated in the FESEM image (Figure 8a) of the orange-red compound. Throughout formation of rodlike nanostructures were observed in place of entangled networks. Shinkai et al.[29] has also reported a morphological alteration in a naphthalenediimide-based organogel system when it is exposed to dihydroxynaphthalene molecules.

In addition, the EDAX and elemental mapping analyses (Figure 8b, c) of the thoroughly washed dried material showed the presence of considerable amount of oxygen along with the others (Cu, N, C, S, and Cl) indicating the possible presence of the acid within the material. This result also authenticates the material as not simply cupric picrate or thioureium picrate but a composite of the metal–ligand complex and picric acid. The material was further characterized with DRS, FTIR, and XRD analyses where in all cases it shows a spectroscopic response, distinct from the picric acid and the pristine gel.

dx.doi.org/10.1021/am501491u | ACS Appl. Mater. Interfaces 2014, 6, 6308–6316

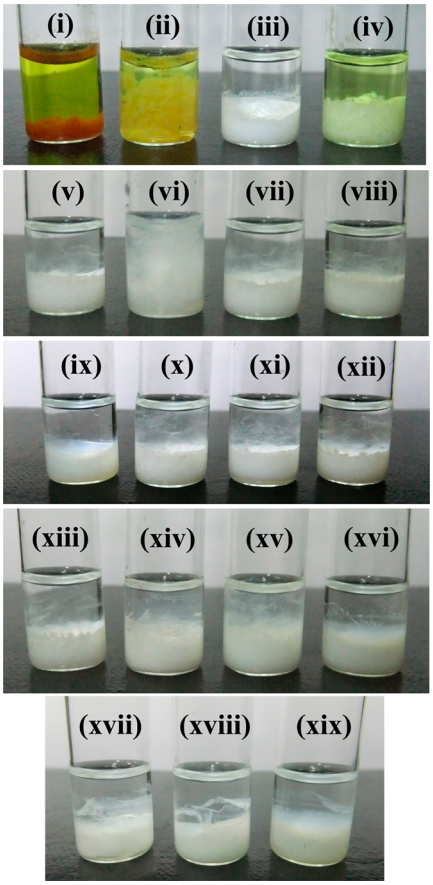

Figure 6. Metallogel incubated with 0.01 M ethanolic solution of 19 different electron deficient probe molecules ((i) picric acid, (ii) 3,5-dinitrosalicylic acid, (iii) 4-nitrobenzaldehyde, (iv) 2,4-dinitropheno,l (v) 4-nitrobenzoic acid, (vi) phthalic acid, (vii) 4-nitrophenol, (viii) 1,3-dinitrobenzene, (ix) 3-nitrophthalic acid, (x) 2-nitrotoluene, (xi) nitrobenzene, (xii) nitromethane, (xiii) benzoic acid, (xiv) salicylic acid, (xv) 3-nitrobenzoic acid, (xvi) 2,4-dinitrotoluene, (xvii) 4-nitrophenyl acetic acid, (xviii) 2-nitropropane, and (xix) 4-nitro-toluene). Formation of orange-red precipitate is clearly visible only for picric acid.

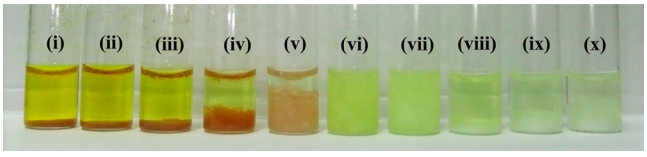

Figure 7. Naked-eye response of the metallogel when incubated with picric acid solution having continuous concentration variation (From set i to x: 5×10^{-2} M, 2.5×10^{-2} M, 1.0×10^{-2} M, 5×10^{-3} M, 2.5×10^{-3} M, 1.0×10^{-3} M, 5×10^{-4} M, 2.5×10^{-4} M, 1.0×10^{-4} M, and 5×10^{-5} M).

In the DRS spectrum (see Figure S13a in the Supporting Information), we observed a broad absorption band having maxima ~470 nm for the samples, whereas picric acid has no such absorption in this region.

Similarly, the 3106 cm^{-1} band, the O−H stretching mode of picric acid, is not observed in the FTIR spectra of those materials (see Figure S13b in the Supporting Information). Therefore, the phenolic proton is expected to be transferred in the thiourea derived gel framework and this proton transfer equilibrium is highly favored by the amine functional mostly abundant within the framework. This is also evident from the blue-shift of the N−H stretching modes observed in the higher wavenumber window for the said materials compared to the xerogel. Similar shift is also reflected in the N−H bending modes. On the other hand, both the symmetric and asymmetric stretching modes of the nitro group shifts to lower wavenumber in the materials compared to picric acid indicating a substantial increase in electron density in the picric acid moiety. It is now expected that the intercalated acid molecules remain present in the supramolecular network as picrate ion and are therefore engaged in extensive hydrogen bonding interactions, which in turn weaken the hydrogen bondings present within the gel scaffold. This seizing of weak force interactions from the gel framework presumably caused the morphological alteration from entangled fibers to rodlike nanostructures.

Again in the XRD profiles (see Figure S13c in the Supporting Information), clear changes were also observed in the diffraction patterns of the materials.

These spectroscopic changes have been reported for some organic picrate salts.[69]

Therefore, this unprecedented selectivity toward only picric acid over the other 18 electron-deficient members could be a consequence of two cooperative mechanisms—the capturing of picric acid molecule within the gel network through proton transfer pathway followed by a charge transfer from the metallogel (donor) to the picric acid (acceptor). To make an in-depth mechanistic study for the interaction of the gel with picric acid, we have performed the sensing study with 2, 4, 6-trinitro-1-chlorobenzene (picryl chloride). Surprisingly, no visual color change was noticed and the gel phase remained unaltered. Though picryl chloride is highly electron-deficient but it has no transferable proton. On the other hand we have already observed no visual change with only acidic probes (which are not highly electron deficient) like 3,5-dinitrosalicylic acid, 3-nitrophthalic acid etc. These clearly suggest that the interaction was highly selective for picric acid only. It is presumable that picric acid first transfers its proton to the gel matrix (which is preferred through the amine groups present in the gel network structure as already discussed) and such proton transfer helps its (PA) entry into the gel network through hydrogen bonding and electrostatic interaction which is then followed by charge transfer from the electron-rich gel matrix to the highly electron-deficient trinitro-backbone of picric acid. Therefore, the proton transfer from picric acid to the gel matrix followed by charge transfer from the gel matrix to the electron deficient picric acid moiety-both are the essential steps for the distinct visual change. Other electron deficient probes could not support this synergistic effect and hence no color change is observed. This proposition could be supported from the observed analytical results (please see Figure 8 and Figure S13 in the Supporting Information). It might also be assumed that, as we got no response in the sensing study with picryl chloride (as mentioned above), trinitro toluene (TNT) is also expected to be unsuccessful in making any change of the gel as we have already observed that the proton transfer from picric acid to the gel is the essential and first step followed by charge transfer for making the visual change (i.e., disruption of the gel with visible color change). As in TNT, there exists no such transferable proton, so the change is also not expected.

Metal−organic coordination complex-based sensing of nitro explosive is comparatively less reported in the literature. With our synthesized gel the naked-eye sensitivity reaches down to 2.5 mM. Here it is worth mentioning that, though this limit is not so impressive in comparison to the detection limit obtained

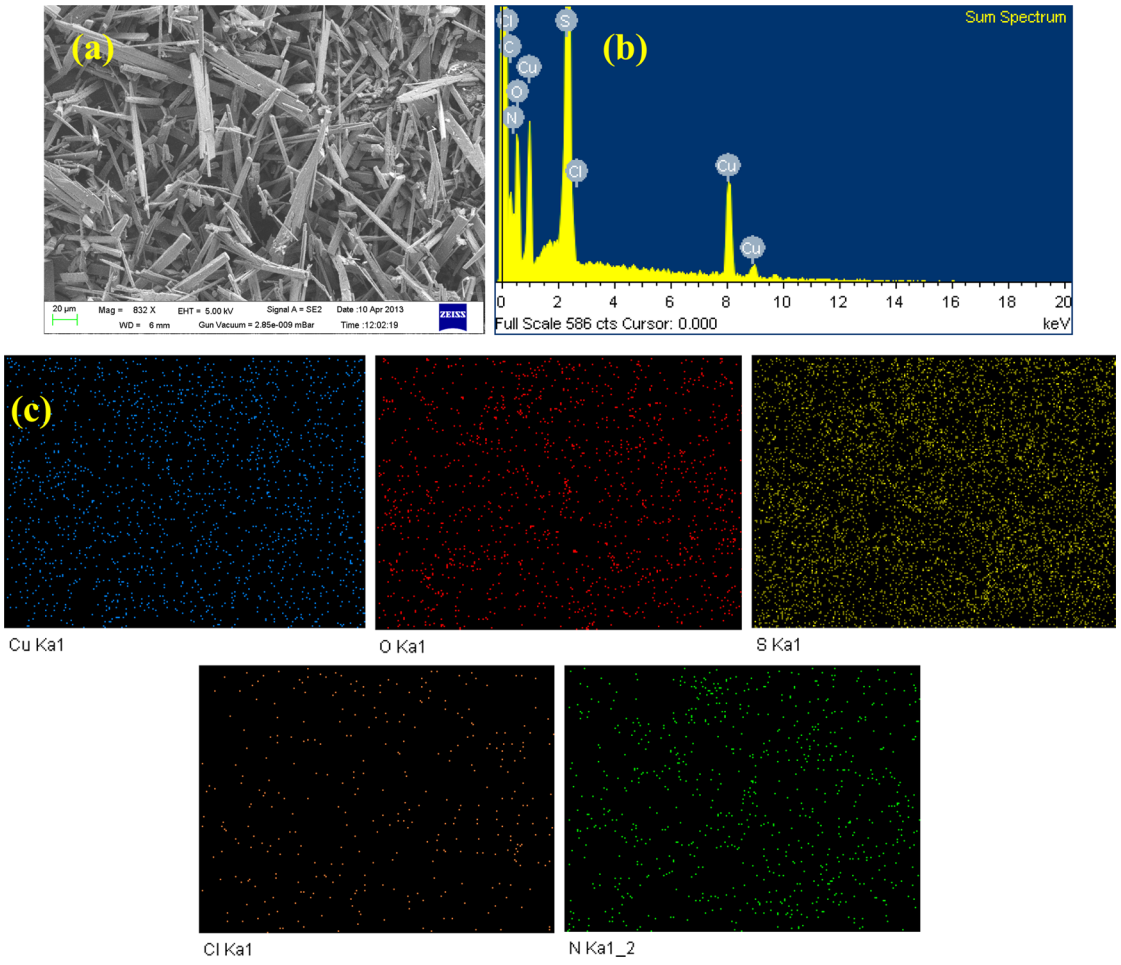

Figure 8. (a) FESEM image of the orange-red precipitate. Throughout, formation of the rodlike morphology clearly indicates morphological change from the fibrous architectures. (b) EDAX pattern and (c) elemental-mapping analysis of the thoroughly washed dried precipitate showing the presence of copper, oxygen, sulfur, chlorine and nitrogen elements in the precipitate. These analyses (b and c) clearly show the presence of oxygen pointing toward the incorporation of picric acid in the gel framework.

in the fluorometric methods of detection of picric acid but the significance of the present MS is the completely naked eye sensing of picric acid circumventing the detection without any instrument. A very recent research article by Garcia et al.[70] has reported the naked eye detection of TNT in aqueous media with sensory polymeric materials down to 1×10^{-2} M. Therefore, our detection limit is conspicuous among the purely naked eye based sensing of picric acid. We have also observed that there occurs no color change when a solution of 2-chloro-1,3,5-trinitrobenzene (picryl chloride) was added in the gel matrix. Therefore, the detection was highly selective toward picric acid. At this concentration (2.5 mM), we observed no distinct visual changes with 3,5-dinitrosalicylic acid and 2, 4-dinitrophenol. However, picric acid imparted distinct color change (orange-red coloration in the gel matrix) at this concentration. Therefore, we may conclude that the as-synthesized gel shows high selectivity toward picric acid only.

The sensing is also observed to operate even in the vapor phase of the acid. Figure 9 presents the color change of the logo (pure air-dried gel) when exposed to picric acid vapor. In our case we have exposed the dried gel made logo to vapors of picric acid for 30 min for getting a sufficient change in the color to make a presentation in the MS (Figure 9) and it was noticed that within 10 min of exposure, a light yellowish color

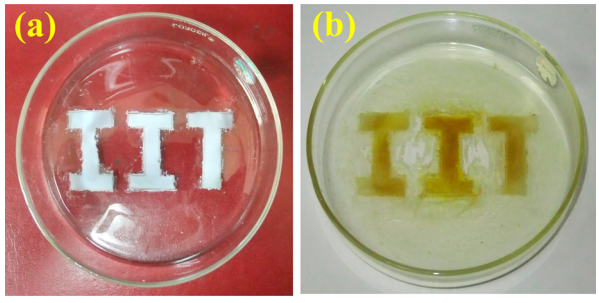

Figure 9. Gel-made "IIT" logo (a) before and (b) after the exposure of picric acid vapor.

developed that distinctly vouches for naked-eye sensing of picric acid in the vapor phase.

This favorable charge transfer from the gel to picric acid is also understandable from the consideration of energies (as calculated by density functional theory[3,19] at the B3LYP/6-31G level) of the LUMOs of all the molecules. From the calculations, we got of the energy of the HOMOs and LUMOs of the molecules (see Table S1 in the Supporting Information). Figure 10 graphically presents the above energy variation for the different molecules. From Figure 10 and Table S1 in the Supporting Information, it is clear that the minimum

dx.doi.org/10.1021/am501491u | ACS Appl. Mater. Interfaces 2014, 6, 6308−6316

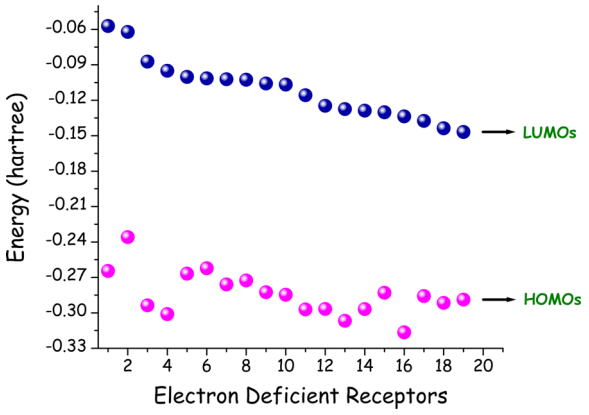

Figure 10. HOMO and LUMO energies (in hartree unit) of the electron deficient analytes employed in the sensing study. The analytes have been arranged in descending order of their corresponding LUMO energy (from left to right: (benzoic acid, aalicylic acid, 2-nitropropane, nitromethane, phthalic acid, 4-nitrophenol, 4-nitrotoluene, 2-nitrotoluene, 4-nitrophenyl acetic acid, nitrobenzene, 3-nitrobenzoic acid, 4-nitrobenzoic acid, 2,4-dinitrotoluene, 3,5-dinitrosalicylic acid, 4-nitrobenzaldehyde, 1,3-dinitrobenzene, 3-nitrophthalic acid, 2,4-dinitrophenol, and picric acid).

LUMO energy is observed for picric acid. Therefore, the charge transfer from the gel matrix is favorable only for picric acid. This favorable charge transfer from the gel matrix to the LUMO of picric acid thus supports the above selectivity. From this theoretical interpretation, it is also understandable that the response is not observed even with 2,4-dinitrophenol, as the LUMO energy of this molecule is higher than the trinitro analogue, i.e., picric acid.

CONCLUSIONS

In conclusion, a Cu(I) metal−organic gel has been fabricated employing two commercially available laboratory chemicals, $CuCl_2$ and thiourea, in water medium. In situ reduction of Cu(II) to Cu(I) with thiourea with subsequent oxidation of the latter to a dithio analogue initiates the formation of the Cu(I) metallogel. It is anticipated that thiourea and the disulfide ligand are largely involved in forming extensive hydrogen bonding through their −N−H protons. Critical analyses of reaction parameters confirm the essential needs of Cu(I) and chloride, both of these ions, to construct the gel framework. And it is also substantiated that simultaneous presence of water is another essential ingredient in the above recipe. The gel is crystalline in nature and shows an entangled fibrous network. The Cu(I) centers make the gel simultaneously fluorescent and redox-responsive. The material gets oxidatively dissolved when treated with $FeCl_3/K_2Cr_2O_7$ and can be again revert back to the gel phase with ascorbic acid. This redox-switchable gel−sol phase transition can be repetitively demonstrated as a highly reproducible event. The reformed gel shows shape persistent characteristics. Other different stimuli (pH, selective metal ions and anions, selective complexing agents etc.) could also assist physicochemical changes in the matrix and thus the synthesized metallogel becomes multiresponsive. Finally, when the white-colored gel was separately exposed to 19 different electron-deficient organic molecules, it selectively acts in response to only picric acid with simultaneous breaking of the gel framework and subsequent formation of an orange-red precipitate. Detailed characterizations of the precipitate corroborate a charge-transfer (CT) mechanism from the donor matrix to the acceptor nitroaromatic, picric acid. A complete change in morphology is also observed from fibrillar networks to rodlike nanostructures. An associated DFT-based theoretical calculations also support the above charge-transfer, having the lowest energy LUMO for picric acid among the LUMOs of the 18 other congeners. Further implementation of this metal−organic coordination gel is under study.

ASSOCIATED CONTENT

Supporting Information

Experimental details; analytical methods; Table S1 (DFT optimized energy of HOMO and LUMO of electron deficient receptors); HOMO−LUMO surfaces of the 19 different molecules; supporting results and figures (FTIR and Raman analyses, FESEM images of the gel for other sets, EDX pattern and elemental analyses of the gel, FESEM image of the xerogel, microscopic images and EDX pattern of the gel obtained from $CuBr_2$, effect of interfering ions, stimuli responsive behavior, pH effect, powder XRD pattern of the dried gel, absorption-emission behavior of the gel, thermogram of the gel, redox switchability of the gel, DRS spectra, FTIR spectra, XRD patterns of picric acid and the orange-red precipitates); rheological results (Figure S14). This material is available free of charge via the Internet at http://pubs.acs.org.

AUTHOR INFORMATION

Corresponding Author

*E-mail: tpal@chem.iitkgp.ernet.in.

Notes

The authors declare no competing financial interest.

ACKNOWLEDGMENTS

The authors are thankful to the CSIR, UGC, DST, and Indian Institute of Technology, Kharagpur, for financial assistance.

REFERENCES

(1) Germain, M. E.; Knapp, M. J. Optical Explosives Detection: From Color Changes to Fluorescence Turn-on. *Chem. Soc. Rev.* **2009**, *38*, 2543−2555.

(2) Salinas, Y.; Agostini, A.; Pérez-Esteve, É.; Martínez-Máñez, R.; Sancenón, F.; Marcos, M. D.; Soto, J.; Costero, A. M.; Gil, S.; Parra, M.; Amorós, P. Fluoregenic Detection of Tetryl and TNT Explosives using Nanoscopic-capped Mesoporous Hybrid Materials. *J. Mater. Chem. A* **2013**, *1*, 3561−3564.

(3) Roy, B.; Bar, A. K.; Gole, B.; Mukherjee, P. S. Fluorescent Tris-Imidazolium Sensors for Picric Acid Explosive. *J. Org. Chem.* **2013**, *78*, 1306−1310.

(4) Tu, R.; Liu, B.; Wang, Z.; Gao, D.; Wang, F.; Fang, Q.; Zhang, Z. Amine-Capped ZnS-Mn^{2+} Nanocrystals for Fluorescence Detection of Trace TNT Explosive. *Anal. Chem.* **2008**, *80*, 3458−3465.

(5) Demirel, G. B.; Daglar, B.; Bayindir, M. Extremely Fast and Highly Selective Detection of Nitroaromatic Explosive Vapours using Fluorescent Polymer Thin films. *Chem. Commun.* **2013**, *49*, 6140−6142.

(6) Sanchez, J. C.; Trogler, W. C. Efficient Blue-emitting Silafluorene-Fluorene-Conjugated Copolymers: Selective Turn-off/Turn-on Detection of Explosives. *J. Mater. Chem.* **2008**, *18*, 3143−3156.

(7) Andrew, T. L.; Swager, T. M. Detection of Explosives via Photolytic Cleavage of Nitroesters and Nitramines. *J. Org. Chem.* **2011**, *76*, 2976−2993.

(8) Freeman, R.; Willner, I. Optical Molecular Sensing with Semiconductor Quantum Dots (QDs). *Chem. Soc. Rev.* **2012**, *41*, 4067−4085.

(9) Mathew, A.; Sajanlal, P. R.; Pradeep, T. Selective Visual Detection of TNT at the Sub-Zeptomole Level. *Angew. Chem., Int. Ed.* **2012**, *51*, 9596−9600.
(10) Bhalla, V.; Arora, H.; Singh, H.; Kumar, M. Triphenylene Derivatives: Chemosensors for Sensitive Detection of Nitroaromatic Explosives. *Dalton Trans.* **2013**, *42*, 969−974.
(11) Riskin, M.; Tel-Vered, R.; Willner, I. Imprinted Au-Nanoparticle Composites for the Ultrasensitive Surface Plasmon Resonance Detection of Hexahydro-1,3,5-trinitro-1,3,5-triazine (RDX). *Adv. Mater.* **2010**, *22*, 1387−1391.
(12) Xu, S.; Lu, H.; Li, J.; Song, X.; Wang, A.; Chen, L.; Han, S. Dummy Molecularly Imprinted Polymers-Capped CdTe Quantum Dots for the Fluorescent Sensing of 2,4,6-Trinitrotoluene. *ACS Appl. Mater. Interfaces* **2013**, *5*, 8146−8154.
(13) Riskin, M.; Tel-Vered, R.; Lioubashevski, O.; Willner, I. Ultrasensitive Surface Plasmon Resonance Detection of Trinitrotoluene by a Bis-aniline-Cross-Linked Au Nanoparticles Composite. *J. Am. Chem. Soc.* **2009**, *131*, 7368−7378.
(14) Dasary, S. S. R.; Singh, A. K.; Senapati, D.; Yu, H.; Ray, P. C. Gold Nanoparticle Based Label-Free SERS Probe for Ultrasensitive and Selective Detection of Trinitrotoluene. *J. Am. Chem. Soc.* **2009**, *131*, 13806−13812.
(15) Filanovsky, B.; Markovsky, B.; Bourenko, T.; Perkas, N.; Persky, R.; Gedanken, A.; Aurbach, D. Carbon Electrodes Modified with TiO_2/Metal Nanoparticles and Their Application for the Detection of Trinitrotoluene. *Adv. Funct. Mater.* **2007**, *17*, 1487−1492.
(16) Kartha, K. K.; Babu, S. S.; Srinivasan, S.; Ajayaghosh, A. Attogram Sensing of Trinitrotoluene with a Self-Assembled Molecular Gelator. *J. Am. Chem. Soc.* **2012**, *134*, 4834−4841.
(17) Vijayakumar, C.; Tobin, G.; Schmitt, W.; Kim, M.-J.; Takeuchi, M. Detection of Explosive Vapours with a Charge Transfer Molecule: Self-assembly Assisted Morphology Tuning and Enhancement in Sensing Efficiency. *Chem. Commun.* **2010**, *46*, 874−876.
(18) Bhalla, V.; Gupta, A.; Kumar, M.; Rao, D. S. S.; Prasad, S. K. Self-Assembled Pentacenequinone Derivative for Trace Detection of Picric Acid. *ACS Appl. Mater. Interfaces* **2013**, *5*, 672−679.
(19) Nagarkar, S. S.; Joarder, B.; Chaudhari, A. K.; Mukherjee, S.; Ghosh, S. K. Highly Selective Detection of Nitro Explosives by a Luminescent Metal−Organic Framework. *Angew. Chem., Int. Ed.* **2013**, *52*, 2881−2885.
(20) Xiao, J.-D.; Qiu, L.-G.; Ke, F.; Yuan, Y.-P.; Xu, G.-S.; Wang, Y.-M.; Jiang, X. Rapid Synthesis of Nanoscale Terbium-based Metal−organic Frameworks by a Combined Ultrasound-vapour Phase Diffusion Method for Highly Selective Sensing of Picric Acid. *J. Mater. Chem. A* **2013**, *1*, 8745−8752.
(21) Liu, K.; Liu, T.; Chen, X.; Sun, X.; Fang, Y. Fluorescent Films Based on Molecular-Gel Networks and Their Sensing Performances. *ACS Appl. Mater. Interfaces* **2013**, *5*, 9830−9836.
(22) Vajpayee, V.; Kim, H.; Mishra, A.; Mukherjee, P. S.; Stang, P. J.; Lee, M. H.; Kim, H. K.; Chi, K.-W. Self-assembled Molecular Squares Containing Metal-based donor: Synthesis and Application in the Sensing of Nitro-aromatics. *Dalton Trans.* **2011**, *40*, 3112−3115.
(23) Samanta, D.; Mukherjee, P. S. Pt^{II}_6 Nanoscopic Cages with an Organometallic Backbone as Sensors for Picric Acid. *Dalton Trans.* **2013**, *42*, 16784−16795.
(24) Dey, N.; Samanta, S. K.; Bhattacharya, S. Selective and Efficient Detection of Nitro-Aromatic Explosives in Multiple Media including Water, Micelles, Organogel, and Solid Support. *ACS Appl. Mater. Interfaces* **2013**, *5*, 8394−8400.
(25) Zhou, X.; Li, L.; Li, H.-H.; Li, A.; Yang, T.; Huang, W. A Flexible Eu(III)-based Metal−organic Framework: Turn-off Luminescent Sensor for the Detection of Fe(III) and Picric acid. *Dalton Trans.* **2013**, *42*, 12403−12409.
(26) Vij, V.; Bhalla, V.; Kumar, M. Attogram Detection of Picric Acid by Hexa-*peri*-Hexabenzocoronene-Based Chemosensors by Controlled Aggregation-Induced Emission Enhancement. *ACS Appl. Mater. Interfaces* **2013**, *5*, 5373−5380.
(27) Liao, Y.; He, L.; Huang, J.; Zhang, J.; Zhuang, L.; Shen, H.; Su, C. − Y. Magnetite Nanoparticle-Supported Coordination Polymer Nanofibers: Synthesis and Catalytic Application in Suzuki-Miyaura Coupling. *ACS Appl. Mater. Interfaces* **2010**, *2*, 2333−2338.
(28) Lee, H.; Jung, S. H.; Han, W. S.; Moon, J. H.; Kang, S.; Lee, J. Y.; Jung, J. H.; Shinkai, S. A Chromo-Fluorogenic Tetrazole-Based $CoBr_2$ Coordination Polymer Gel as a Highly Sensitive and Selective Chemosensor for Volatile Gases Containing Chloride. *Chem.—Eur. J.* **2011**, *17*, 2823−2827.
(29) Mukhopadhyay, P.; Iwashita, Y.; Shirakawa, M.; Kawano, S.; Fujita, N.; Shinkai, S. Spontaneous Colorimetric Sensing of the Positional Isomers of Dihydroxynaphthalene in a 1D Organogel Matrix. *Angew. Chem., Int. Ed.* **2006**, *45*, 1592−1595.
(30) Paul, M.; Adarsh, N. N.; Dastidar, P. Cu^{II} Coordination Polymers Capable of Gelation and Selective SO_4^{-2} Separation. *Cryst. Growth Des.* **2012**, *12*, 4135−4143.
(31) Kar, T.; Debnath, S.; Das, D.; Shome, A.; Das, P. K. Organogelation and Hydrogelation of Low-Molecular-Weight Amphiphilic Dipeptides: pH Responsiveness in Phase-Selective Gelation and Dye Removal. *Langmuir* **2009**, *25*, 8639−8648.
(32) Samanta, S. K.; Bhattacharya, S. Wide-Range Light-Harvesting Donor−Acceptor Assemblies through Specific Intergelator Interactions via Self-Assembly. *Chem.—Eur. J.* **2012**, *18*, 15875−15885.
(33) Babu, S. S.; Praveen, V. K.; Prasanthkumar, S.; Ajayaghosh, A. Self-Assembly of Oligo(*para*-phenylenevinylene)s through Arene-Perfluoroarene Interactions: π Gels with Longitudinally Controlled Fiber Growth and Supramolecular Exciplex-Mediated Enhanced Emission. *Chem.—Eur. J.* **2008**, *14*, 9577−9584.
(34) Roubeau, O.; Colin, A.; Schmitt, V.; Clérac, R. Thermoreversible Gels as Magneto-Optical Switches. *Angew. Chem., Int. Ed.* **2004**, *43*, 3283−3286.
(35) Lee, H.; Lee, J. H.; Kang, S.; Lee, J. Y.; John, G.; Jung, J. H. Pyridine-based Coordination Polymeric Hydrogel with Cu^{2+} ion and its Encapsulation of a Hydrophobic Molecule. *Chem. Commun.* **2011**, *47*, 2937−2939.
(36) Hu, Y.; Fan, Y.; Huang, Z.; Song, C.; Li, G. In situ Fabrication of Metal-Organic Hybrid Gels in a Capillary for Online Enrichment of Trace Analytes in Aqueous Samples. *Chem. Commun.* **2012**, *48*, 3966−3968.
(37) Weiss, R. G.; Terech, P., Eds.; *Molecular Gels: Materials with Self-Assembled Fibrillar Networks*; Springer: Dordrecht, The Netherlands, 2006.
(38) Sangeetha, N. M.; Maitra, U. Supramolecular Gels: Functions and Uses. *Chem. Soc. Rev.* **2005**, *34*, 821−836 and references there-in.
(39) Bhattacharya, S.; Srivastava, S.; Pal, A. Modulation of Viscoelastic Properties of Physical Gels by Nanoparticle Doping: Influence of the Nanoparticle Capping Agent. *Angew. Chem., Int. Ed.* **2006**, *45*, 2934−2937.
(40) Basit, H.; Pal, A.; Sen, S.; Bhattacharya, S. Two-Component Hydrogels Comprising Fatty Acids and Amines: Structure, Properties, and Application as a Template for the Synthesis of Metal Nanoparticles. *Chem.—Eur. J.* **2008**, *14*, 6534−6545.
(41) Antonietti, M.; Gröhn, F.; Hartmann, J.; Bronstein, L. Nonclassical Shapes of Noble-Metal Colloids by Synthesis in Microgel Nanoreactors. *Angew. Chem., Int. Ed.* **1997**, *36*, 2080−2082.
(42) Vemula, P. K.; Aslam, U.; Mallia, V. A.; John, G. In Situ Synthesis of Gold Nanoparticles Using Molecular Gels and Liquid Crystals from Vitamin-C Amphiphiles. *Chem. Mater.* **2007**, *19*, 138−140.
(43) Raeburn, J.; Cardoso, A. Z.; Adams, D. J. The Importance of the Self-assembly Process to Control Mechanical Properties of Low Molecular Weight Hydrogels. *Chem. Soc. Rev.* **2013**, *42*, 5143−5156.
(44) Brizard, A.; Oda, R.; Huc, I. In *Low Molecular Mass Gelators, Design, Self-Assembly, Function*; Fages, F., Ed.; Springer: Berlin, 2005; pp 167−218.
(45) Tam, A. Y.-Y.; Yam, V. W.-W. Recent Advances in Metallogels. *Chem. Soc. Rev.* **2013**, *42*, 1540−1567 *and references there-in.*
(46) Imaz, I.; Rubio-Martínez, M.; Saletra, W. J.; Amabilino, D. B.; Maspoch, D. Amino Acid Based Metal-Organic Nanofibers. *J. Am. Chem. Soc.* **2009**, *131*, 18222−18223.

(47) Odriozola, I.; Loinaz, I.; Pomposo, J. A.; Grande, H. J. Gold-glutathione Supramolecular Hydrogels. *J. Mater. Chem.* **2007**, *17*, 4843−4845.
(48) Casuso, P.; Carrasco, P.; Loinaz, I.; Cabañero, G.; Grande, H. J.; Odriozola, I. Argentophilic Hydrogels: Elucidating the Structure of Neutral *versus* Acidic Systems. *Soft Matter* **2011**, *7*, 3627−3633.
(49) Banerjee, S.; Kandanelli, R.; Bhowmik, S.; Maitra, U. Self-organization of Multiple Components in a Steroidal Hydrogel Matrix: Design, Construction and Studies on Novel Tunable Luminescent Gels and Xerogels. *Soft Matter* **2011**, *7*, 8207−8215.
(50) Bairi, P.; Roy, B.; Nandi, A. K. pH and Anion Sensitive Silver(I) Coordinated Melamine Hydrogel with Dye Absorbing Properties: Metastability at Low Melamine Concentration. *J. Mater. Chem.* **2011**, *21*, 11747−11749.
(51) Saha, S.; Schön, E.-M.; Cativiela, C.; Díaz, D. D.; Banerjee, R. Proton-Conducting Supramolecular Metallogels from the Lowest Molecular Weight Assembler Ligand: A Quote for Simplicity. *Chem.—Eur. J.* **2013**, *19*, 9562−9568.
(52) Sarkar, S.; Pradhan, M.; Sinha, A. K.; Basu, M.; Pal, T. Selective and Sensitive Recognition of Cu^{2+} in an Aqueous Medium: A Surface-Enhanced Raman Scattering (SERS)-Based Analysis with a Low-Cost Raman Reporter. *Chem.—Eur. J.* **2012**, *18*, 6335−6342.
(53) Segarra-Maset, M. D.; Nebot, V. J.; Miravet, J. F.; Escuder, B. Control of Molecular Gelation by Chemical Stimuli. *Chem. Soc. Rev.* **2013**, *42*, 7086−7098.
(54) Maeda, H. Anion-Responsive Supramolecular Gels. *Chem.—Eur. J.* **2008**, *14*, 11274−11282.
(55) Kawano, S. −i.; Fujita, N.; Shinkai, S. A Coordination Gelator That Shows a Reversible Chromatic Change and Sol-Gel Phase-Transition Behavior upon Oxidative/Reductive Stimuli. *J. Am. Chem. Soc.* **2004**, *126*, 8592−8593.
(56) Liu, J.; He, P.; Yan, J.; Fang, X.; Peng, J.; Liu, K.; Fang, Y. An Organometallic Super-Gelator with Multiple-Stimulus Responsive Properties. *Adv. Mater.* **2008**, *20*, 2508−2511.
(57) He, Y.; Bian, Z.; Kang, C.; Cheng, Y.; Gao, L. Chiral Binaphthylbisbipyridine-based Copper(I) Coordination Polymer Gels as Supramolecular Catalysts. *Chem. Commun.* **2010**, *46*, 3532−3534.
(58) Miao, W.; Zhang, L.; Wang, X.; Cao, H.; Jin, Q.; Liu, M. A Dual-Functional Metallogel of Amphiphilic Copper(II) Quinolinol: Redox Responsiveness and Enantioselectivity. *Chem.—Eur. J.* **2013**, *19*, 3029−3036.
(59) Bombicz, P.; Mutikainen, I.; Krunks, M.; Leskelä, T.; Madarász, J.; Niinistö, L. Synthesis, Vibrational Spectra and X-ray Structures of Copper(I) Thiourea Complexes. *Inorg. Chim. Acta* **2004**, *357*, 513−525.
(60) Bhattacharya, S.; Samanta, S. K. Soft Functional Materials Induced by Fibrillar Networks of Small Molecular Photochromic Gelators. *Langmuir* **2009**, *25*, 8378−8381.
(61) Piepenbrock, M.-O. M.; Clarke, N.; Steed, J. W. Rheology and Silver Nanoparticle Templating in a Bis(urea) Silver Metallogel. *Soft Matter* **2011**, *7*, 2412−2418.
(62) Steed, J. W. Anion-tuned Supramolecular Gels: A Natural Evolution from Urea Supramolecular Chemistry. *Chem. Soc. Rev.* **2010**, *39*, 3686−3699.
(63) Esch, J. H. v.; Schoonbeek, F.; Loos, M. d.; Kooijman, H.; Spek, A. L.; Kellogg, R. M.; Feringa, B. L. Cyclic Bis-Urea Compounds as Gelators for Organic Solvents. *Chem.—Eur. J.* **1999**, *5*, 937−950.
(64) George, M.; Tan, G.; John, V. T.; Weiss, R. G. Urea and Thiourea Derivatives as Low Molecular-Mass Organogelators. *Chem.—Eur. J.* **2005**, *11*, 3243−3254.
(65) Džolić, Z.; Cametti, M.; Milić, D.; Žinić, M. The Formation of $CuCl_2$-Specific Metallogels of Pyridyloxalamide Derivatives in Alcohols. *Chem.—Eur. J.* **2013**, *19*, 5411−5416.
(66) Lee, J. H.; Kang, S.; Lee, J. Y.; Jung, J. H. A Tetrazole-based Metallogel Induced with Ag^+ ion and its Silver Nanoparticle in Catalysis. *Soft Matter* **2012**, *8*, 6557−6563.
(67) Piepenbrock, M.-O. M.; Lloyd, G. O.; Clarke, N.; Steed, J. W. Metal- and Anion-binding Supramolecular Gels. *Chem. Rev.* **2010**, *110*, 1960−2004.
(68) Fatás, P.; Bachl, J.; Oehm, S.; Jiménez, A. I.; Cativiela, C.; Díaz, D. D. Multistimuli-Responsive Supramolecular Organogels Formed by Low-Molecular-Weight Peptides Bearing Side-Chain Azobenzene Moieties. *Chem.—Eur. J.* **2013**, *19*, 8861−8874.
(69) Dhanabal, T.; Amirthaganesan, G.; Dhandapani, M.; Das, S. K. Spectral, Crystal Structure, Thermal and Antimicrobial Characterisation of an Organic Charge Transfer Complex 3,5-dimethylpyrrazolinium Picrate. *J. Mol. Struct.* **2013**, *1035*, 483−492.
(70) Pablos, J. L.; Trigo-López, M.; Serna, F.; García, F. C.; García, J. M. Water-soluble Polymers, Solid Polymer Membranes, and Coated Fibres as Smart Sensory Materials for the Naked Eye Detection and Quantification of TNT in Aqueous Media. *Chem. Commun.* **2014**, *50*, 2484−2487.